Article

Strain Rate and Temperature Effects on Formability and Microstructure of AZ31B Magnesium Alloy Sheet

Song Xue [1,2,*], Tao Yang [1,2], Xuedong Liu [1,2], Yi Ren [1,2], Yi Peng [1,2] and Lixuan Zheng [1,2]

1   School of Manufacturing and Science Engineering, Southwest University of Science and Technology, Mianyang 621010, China; yangtaoctu@163.com (T.Y.); liuxuedong1107@163.com (X.L.); nrenyi0829@163.com (Y.R.); jovita1998@163.com (Y.P.); xuesongcd@163.com (L.Z.)
2   Key Laboratory of Testing Technology for Manufacturing Process, Ministry of Education, Southwest University of Science and Technology, Mianyang 621010, China
*   Correspondence: xuesong2004@126.com; Tel.: +86-0816-6089-685

Abstract: Magnesium alloys play an important role in lightweight structures, which are extensively used in different industries due to their excellent mechanical and physical properties. In this paper, the formability of the AZ31B magnesium alloy sheet was studied by using tensile tests at different temperatures (from 25 to 250 °C) and strain rates (from 0.017 s^{-1} to 0.34 s^{-1}). The results showed that the material behaves with positive temperature sensitivity when forming at a temperature lower than 200 °C. The effect of the strain rates on the formability of AZ31B was larger at high temperatures. The metallography of AZ31B at different temperatures and strain rates was observed by OM. The results showed that the partially recrystallized structure was exhibited at a temperature of 150 °C. With the increase in temperature, the approximate complete recrystallization was exhibited at a temperature of 250 °C. The fracture morphology of AZ31B was observed at different strain rates and temperatures by SEM. Additionally, the main fracture pattern was quasi-cleavage at room temperature. However, with the increase in temperature, the fracture pattern was transited from a quasi-cleavage pattern to a ductile fracture pattern. The ductile fracture pattern was the main fracture pattern at a temperature of 250 °C.

Keywords: strain rate; temperature; AZ31B magnesium alloy; formability

1. Introduction

With the increase in energy demands and environmental pressure, many researchers and manufacturers find that declining the weight of a vehicle plays an important role in protecting the environment and improving the efficiency of fuel consumption [1,2]. Declining the weight of a vehicle is the key issue when it is designed in the future. Therefore, it is imperative to develop lightweight metal materials to replace the traditional metal materials in the automotive applications field [3]. In order to achieve this goal, some research groups have been investigating some lightweight metal materials to fabricate the components of vehicles, such as aluminum alloy or magnesium alloy [4].

Magnesium (Mg) alloy is a special lightweight-structure metal material, and it exhibits distinctive properties from other metals in terms of mechanical property (e.g., traditional metal, steel and aluminum alloy) [5–7]. In recent years, magnesium alloys have been extensively used in industrial fields (e.g., aerospace, automotive manufacturing, electronic communications, military affairs, nuclear power) due to their unique mechanical properties, such as low density, high specific stiffness and high specific strength and easy recovery. However, the poor plasticity and formability of magnesium alloy sheets are exhibited at room temperature due to their special crystal structure (the hexagonal closed-packed crystal structure, with few slip systems and a strong basal plane texture) [8]. Through the research of William J. Joost [9], the results showed that magnesium alloy exhibits tremendous potential in the industrial field, but some technical barriers limit its development. The

AZ-series magnesium alloy is one of the magnesium alloys with a high aluminum content, which is widely used in industrial applications based on its high strength, high ductility and so on. At present, the AZ31B magnesium alloy is considered to be the one with the most potential for magnesium alloy in structural applications based on the Mg–Al–Zn ternary system [10].

Tensile testing is the most important method used to analyze the formability, plasticity and mechanical properties of metal sheets. The material's characteristics can be obtained when a specimen is stretched until it is broken, such as its strain at break, yield strength, Young's modulus and ultimate tensile strength, etc. [11]. Zihan Li et al. [12] investigated the formability of AZ31B magnesium alloy sheet at an elevated temperature. The analysis results showed that the forming limit of AZ31B was improved by increasing the forming temperature. Zimin Wang et al. [13] investigated the effects of temperature for the up die on the formability of AZ31B magnesium alloy in the forming process. The analysis results showed that the formability of AZ31B could be improved by increasing the upper-die temperature during the stamping process. Wurong Wang et al. [14] studied the formability of AZ31B magnesium alloy in the warm-stamping process. The studied results showed that the stamping formability of material could be seriously influenced by the changing temperature during the warm-stamping process, and the serious anisotropy emerged when the temperature was raised to 250 °C. D. Ghaffari et al. [15] investigated the effects of the temperature gradient and the strain rate on the formability of AZ31B magnesium alloy and the results showed that the formability of the material could be improved considerably by increasing the temperatures and the effects of the stain rates in the forming process and was enhanced with the raising of temperatures. Xi Nie et al. [16] studied the effects of isothermal compression on the microstructural evolution of AZ31B magnesium alloy. The results showed that the grain structure of AZ31B could be refined effectively by increasing the deformation extent and cooling rate during the hot process, and the mechanical property was improved by controlling the size of the grains of material. Jing-Ren Dong et al. [17] studied the critical damage value of AZ31B magnesium alloy by tensile test under different temperatures and strain rates. They obtained that the critical damage values were more sensitive to the deformation temperature. Zhou Guowei et al. and Wang HM et al. [18,19] investigated the strain-rate sensitivities of AZ31B magnesium alloy at various temperatures through tensile tests and numerical simulation. The results showed that anisotropy illustrates a larger dependence on the strain rate. Considering the effects of tool temperature on the formability of AZ31B, Guang-sheng HUANG et al. [20] investigated the forming limit diagrams (FLDs) of AZ31B magnesium alloy sheet by conducting stretch-forming tests at different temperatures. They concluded that the reduction of texture intensity is effective to the improvement of formability not only at room temperature but also at low-and-medium temperature. But effect of texture on FLDs becomes weak with increasing temperature. De-Hua Yu [21] studied the elevated temperature deformation behavior of AZ31B from the point of view of modeling and constitutive. According to the previous study about AZ31B, similar studies provided some guidance for this article. However, the effects of the multiple strain rates and temperatures at the same time were not investigated in the tensile process. Therefore, according to the demand for industry components of AZ31B, it is with great significance that we study the formability of AZ31B magnesium alloy sheet at different strain rates and forming temperatures.

In this article, the formability of the AZ31B magnesium alloy sheet was studied under the multiple strain rates and tensile temperatures. The optimum formability of the AZ31B magnesium alloy sheet was considered based on the analysis of its mechanical properties and microstructure. Meanwhile, some guidance has been provided to help others who study the formability of AZ31B magnesium alloy sheets in the future.

2. Materials and Methods

2.1. Material and Sample Design

A thickness of 1.2 mm commercial AZ31B magnesium alloy sheet was selected as the analysis material in this study. This material is a type of wrought magnesium alloy, which was produced by squeeze casting. The chemical composition of the material is listed in Table 1.

Table 1. Chemical composition of AZ31B magnesium alloy sheet (wt%. mass fraction).

Element	Mg	Al	Si	Ca	Zn	Mn	Fe	Cu	Ni
Standard value	bal.	2.420	0.080	0.040	1.020	0.300	0.003	0.010	0.001

The specimens were prepared according to the GB/T 228.1–2010 metallic materials test pieces for tensile testing [22]. The specimens' sampling direction, the material's rolling direction, and the specimen's size are shown in Figure 1.
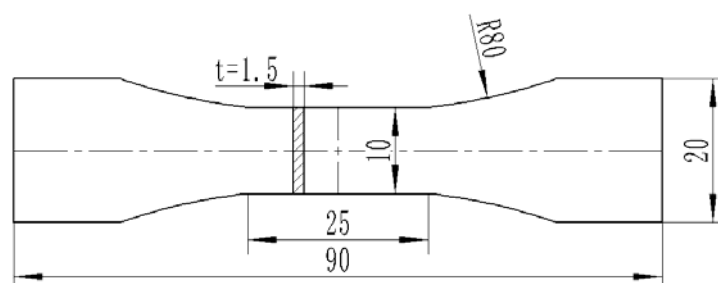

Figure 1. The sketch drawing of tensile testing specimens (unit: mm).

2.2. Experimental Methods

In order to keep the stability of the temperature during the experiment process, the tensile tests' equipment was carried out by using the MTS, as shown in Figure 2. The MTS was equipped with a controllable environmental chamber, which was heated by a hot air blower motor. Based on the manufacturing process and the formability of the AZ31B magnesium alloy sheet's structural parts, the tensile test temperatures selected were 25 °C, 150 °C, 200 °C, and 250 °C, and the strain rates selected were 0.017 s^{-1}, 0.17 s^{-1}, 0.34 s^{-1}, as shown in Figure 3. These tensile temperatures and rates were mostly contained within the range of the AZ31B magnesium alloy sheet industrial-forming conditions [23]. Before the tensile testing, the specimens remained in the testing environment temperature for 30 min. According to the records of the load distributions relationship of the positions and loads in the tensile process, the true stress and true strain were calculated. The same experimental conditions for the specimens were repeated five times to ensure the reliability of the results. After the tensile testing, the microstructures of the specimens were analyzed by OM (optical microscope) and SEM (scanning electron microscopy).

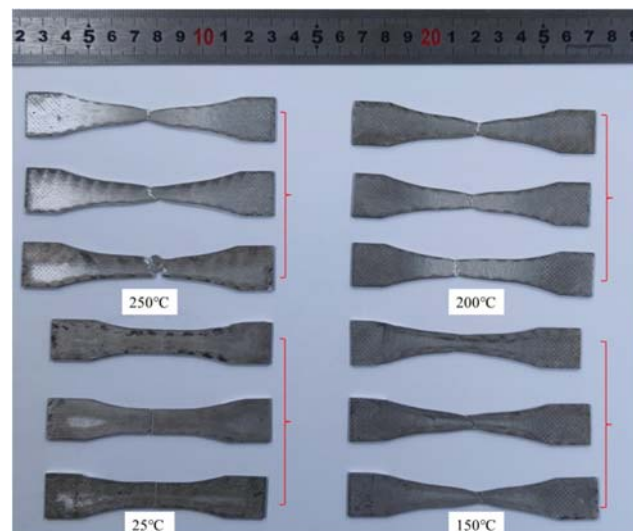**Figure 2.** The MTS tensile testing system with a controllable environmental chamber.

Figure 3. Specimens after tensile testing.

3. Results and Discussion

3.1. Mechanical Property

The data of the true stress and true strain of the tensile tests of AZ31B under the different strain rates at each experiment temperature are shown in Figure 4. In the experiment process, $0.017 \, \text{s}^{-1}$ was the slowest strain rate, and $0.34 \, \text{s}^{-1}$ was the fastest strain rate at each experimental temperature. The strain rate was the most important factor in affecting the plasticity and formability of the AZ31B magnesium alloy sheet based on the exhibition of the test data. According to the analysis of data, the results showed that the lower effect of the strain rate on formability was exhibited at a lower temperature, as shown in Figure 4a.

At a temperature of 25 °C, the deviation value of true stress between the maximum strain rate and minimum strain rate was 76 MPa when the true strain rose to 0.2. With the increase in the temperature, the effect of the strain rate on the formability of AZ31B was increased, as shown in Figure 4b–d. At a temperature of 250 °C, the deviation value of true stress between the maximum strain rate and minimum strain rate was 118 MPa when the true strain rose to 0.2. Additionally, the growth rate of the true stress was 55%, from 25 °C to 250 °C, as shown in Figure 5. Therefore, the effect of the strain rate on the formability of AZ31B increased at a high temperature.
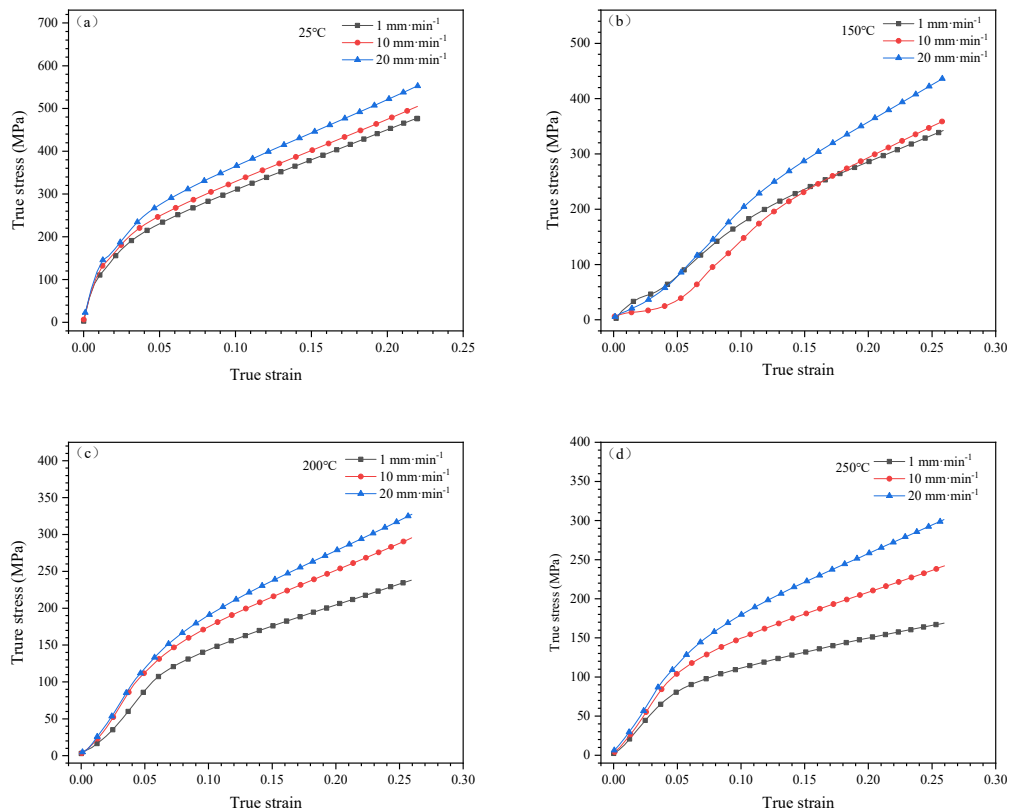

Figure 4. The true stress and true strain of AZ31B under the different strain rates at each experiment temperature. (**a**) at 25 °C; (**b**) 150 °C; (**c**) at 200 °C; (**d**) at 250 °C.
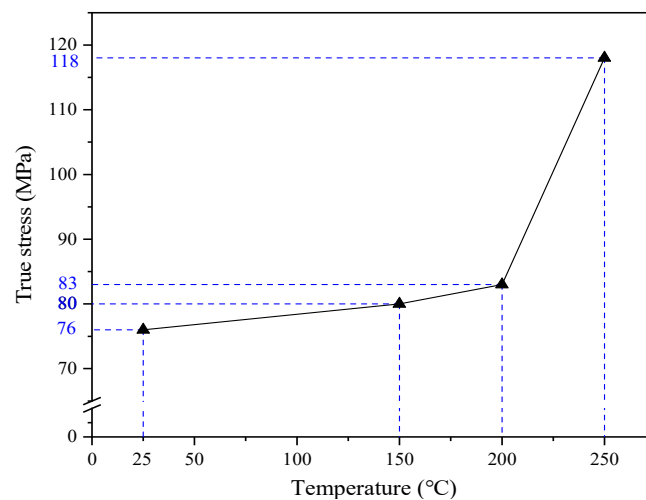

Figure 5. The deviation value of true stress on the true strain of 0.2 at different tensile temperatures.

Through the analysis above, the temperature was also an important factor in improving the formability of the AZ31B magnesium alloy sheet during the forming process. The data of true stress and true strain at the different temperatures under each experiment strain rate is shown in Figure 6. Based on the analysis of experimental data under each strain rate, the results showed that there was a serious effect of the temperature on the formability of AZ31B. In a constant strain-rate state, the true stress of AZ31B was seriously reduced with an increase in the temperature. Additionally, the percentage elongation after the fracture of AZ31B at different temperatures and strain rates is shown in Figure 7. According to the data analysis on the percentage elongation after a fracture, the results showed that there was a lower effect of strain rate on the plasticity of AZ31B at a temperature of 25 °C. With the increase in temperature during the tensile process, the effect of the strain rate on the plasticity of AZ31B was increased. Meanwhile, the plasticity of AZ31B was improved with the increase in temperature under the constant strain rate.
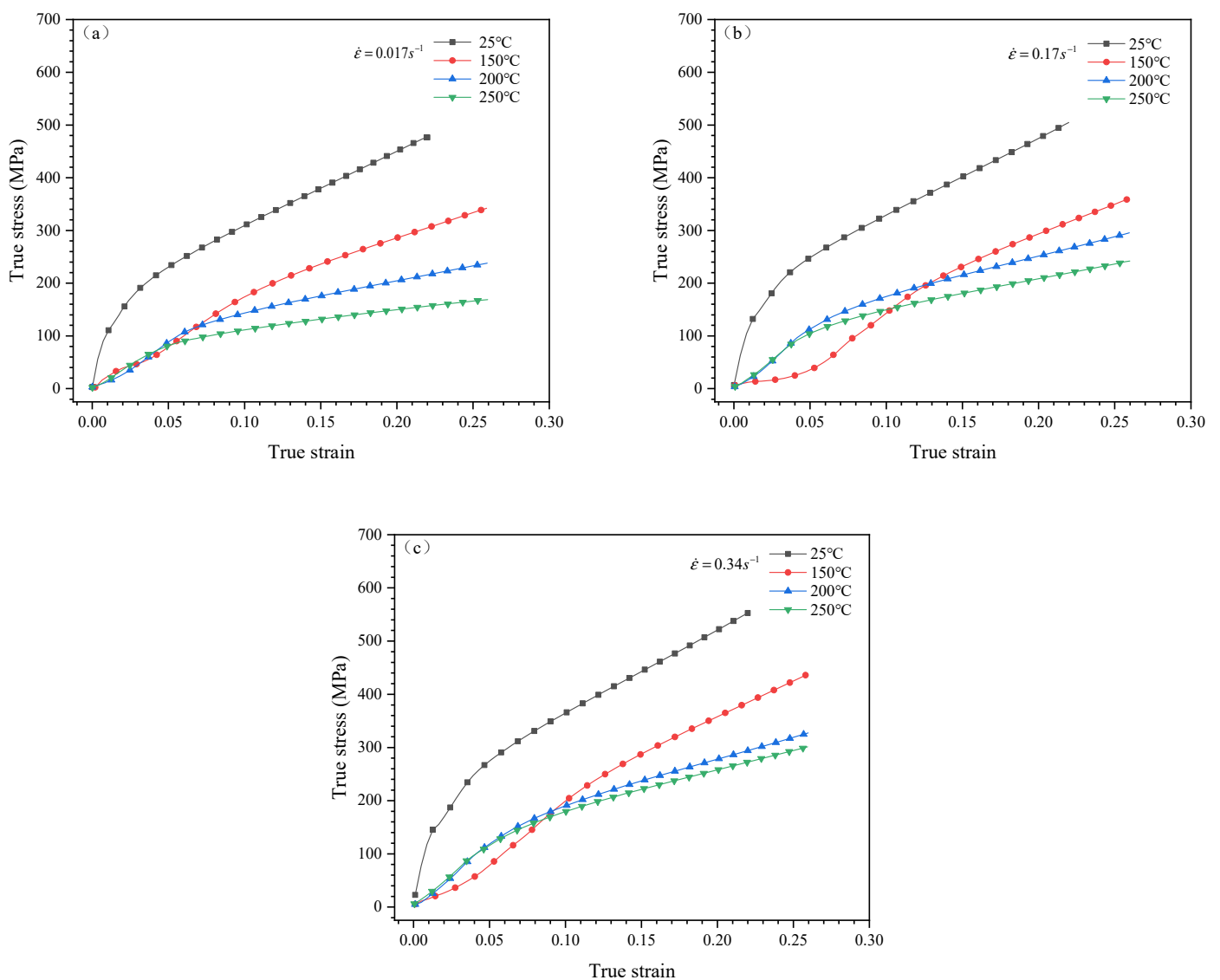

Figure 6. The true stress and true strain of AZ31B at different experiment temperatures under each strain rate. (**a**) $\dot{\varepsilon} = 0.017$ s^{-1}; (**b**) $\dot{\varepsilon} = 0.17$ s^{-1}; (**c**) $\dot{\varepsilon} = 0.34$ s^{-1}.
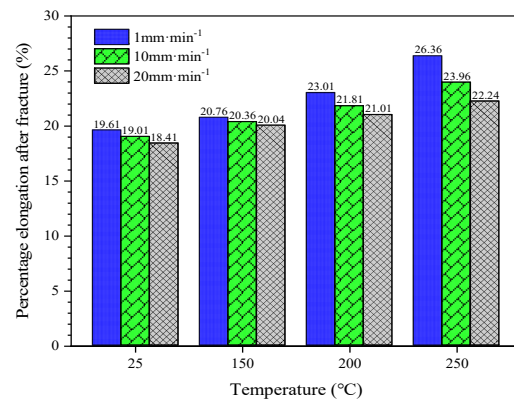
Figure 7. The percentage elongation after fracture of AZ31B at the different tensile temperatures and rates.

The reason for this phenomenon was that the formability of AZ31B was mainly determined based on the competing hardening and softening [24]. At the lower temperature, the density of dislocation increased and proliferated rapidly during the deformation process, which caused the dislocation movement to become more and more difficult. The hardening played a major role during the tensile process at room temperature. Therefore, the poor effect of strain rate on the formability was exhibited. Furthermore, a lower percentage of elongation after the fracture and plasticity occurred was exhibited. However, the competition between the hardening and softening changed with the increase in temperature. At the high temperature, the dislocation movement was improved due to enough energy in the deformation process [25,26]. The softening played a major role during the tensile process. Therefore, a higher percentage of elongation after AZ31B's fracture and plasticity was exhibited at the high temperature. In addition, at the high strain rate, there was not enough time for the plasticity deformation, so the lower plasticity and formability of AZ31B were exhibited.

3.2. Microstructure Evolution

The primary metallography of AZ31B magnesium alloy at room temperature was shown and was not an obvious characteristic of the elongated and recrystallised grains, as shown in Figure 8. The size-uniformity of the grains was observed, and the average grain size was 15.8 μm. At a temperature of 25 °C, under the lower strain rate, no obvious characteristics were observed for the deformation of the structure of the grain, and the relatively uniform structure of the grain was observed, as shown in Figure 9a,b. However, when the strain rate rose to 0.34 s^{-1}, the slight feature of elongation for the grain was observed, as shown in Figure 9c. It was stressed when the lower effect of the strain rate on the deformation of the grain structure was at room temperature.
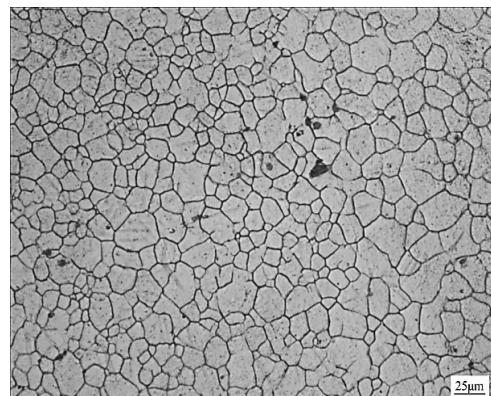

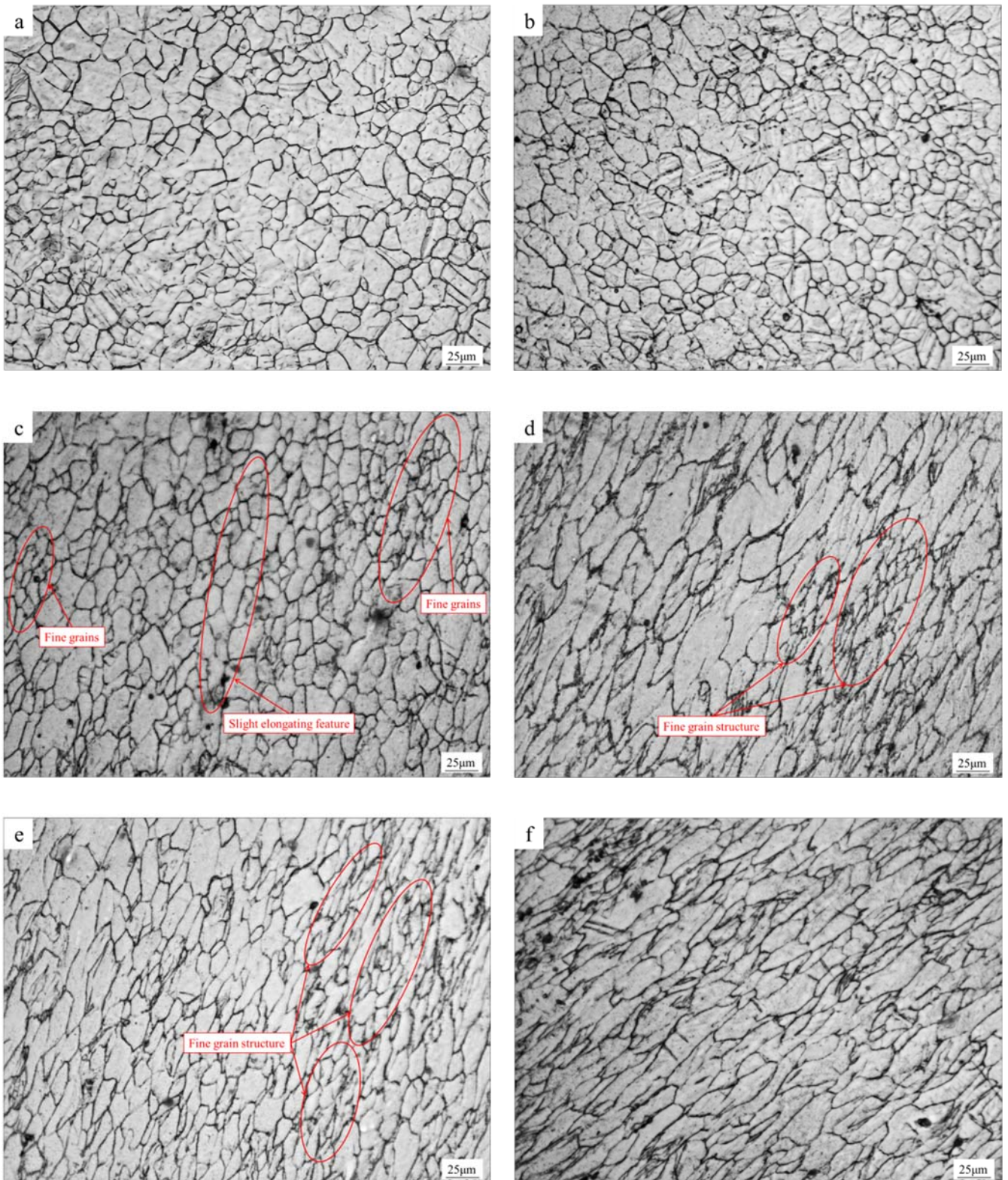**Figure 8.** The metallography of the AZ31B magnesium alloy sheet at 25 °C.
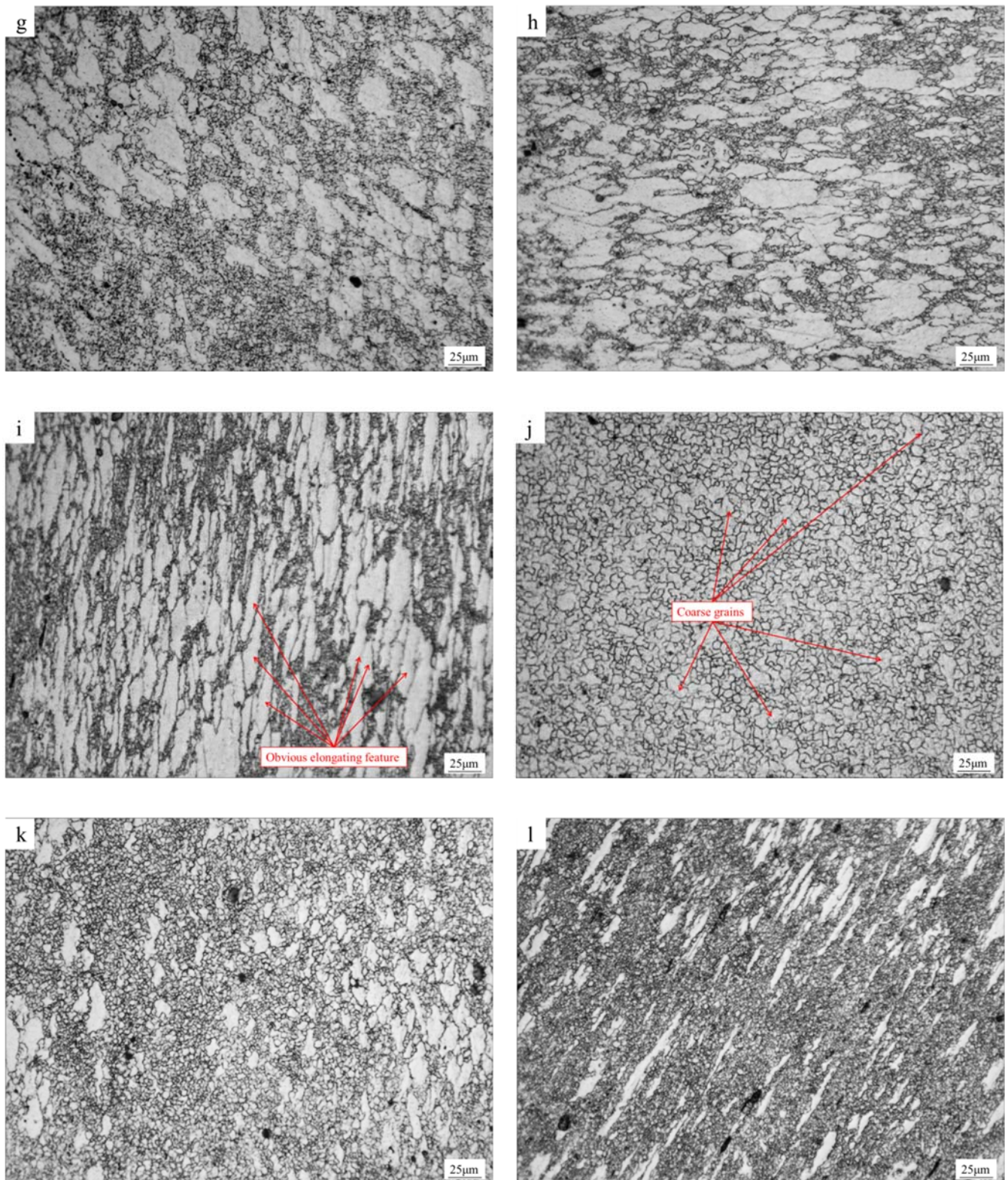
Figure 9. *Cont*.

Figure 9. The metallography of AZ31B at different temperatures and strain rates. (**a**) 0.017 s^{-1} at 25 °C; (**b**) 0.17 s^{-1} at 25 °C; (**c**) 0.34 s^{-1} at 25 °C; (**d**) 0.017 s^{-1} at 150 °C; (**e**) 0.17 s^{-1} at 150 °C; (**f**) 0.34 s^{-1} at 150 °C; (**g**) 0.017 s^{-1} at 200 °C; (**h**) 0.17 s^{-1} at 200 °C; (**i**) 0.34 s^{-1} at 200 °C; (**j**) 0.017 s^{-1} at 250 °C; (**k**) 0.17 s^{-1} at 250 °C; (**l**) 0.34 s^{-1} at 250 °C.

With the increase in temperature, the deformation degree of grains was gradually increased, and the grains were elongated in the tensile direction, as shown in Figure 9d–i.

When the temperature was raised to 150 °C, the shapes of the grain were deformed from an equiaxed shape to a flat shape, and the deformation degree of the shape of grains was increased with the increase in strain rate. Meanwhile, there were some fine grains observed, which were considered the initial stage of recrystallization of AZ31B, as shown in Figure 9d,e. When the temperature was raised to 200 °C, the recrystallization degree was increased, and more fine-grain structures were observed, as shown in Figure 9g–i. The effect of the strain rate on the grain structure was increased at high temperatures. Under the lower strain rate, the grains were mainly divided into a fine grain and coarse grain, and the coarse grains were not obviously elongated, as shown in Figure 9g. However, when the strain rate rose to 0.34 s^{-1}, the obvious elongation feature for coarse grains was observed, as shown in Figure 9i. When the temperature was raised to 250 °C, the obvious characteristics of an approximate complete recrystallization and relative uniform fine-grain structure were observed. The average grain size was 9.8 μm. However, there were also a few coarse grains observed, as shown in Figure 9j. Additionally, the approximate spiculate morphology of the coarse grains was observed when the strain rate rose to 0.34 s^{-1}, as shown in Figure 9l. According to the analysis above, at the high temperature, with an increase in the strain rate, the degree of elongating for the coarse grains gradually increased. The average grain size was reduced, and the recrystallization increased continually with the increase in temperature. Additionally, the more serious effect of the high strain rate on the grain structure was exhibited at the high temperature, as shown in Figure 9c,f,i,l. Therefore, the better plasticity and uniform fine-grain structure of the AZ31B magnesium alloy sheet could be obtained under the lower strain rate at the higher temperature.

As shown in Figure 10, the typical fracture morphology of the AZ31B specimens under the different temperatures and strain rates was observed by SEM. The fracture morphology of AZ31B under the different strain rates at a temperature of 25 °C is shown in Figure 10a–c. According to the analysis of the fracture pattern, the cleavage steps and the river pattern were the main fracture patterns at this experimental temperature. At a temperature of 25 °C, with the increase in the strain rate, the fracture morphology was mainly composed of cleavage steps to the river pattern. There was quite a difference with other light metals in the fracture model under the high strain rate [27]. The increase in the temperature and the fracture morphology of AZ31B under the different strain rates is shown in Figure 10d–i. The quasi-cleavage river pattern was observed in the fracture morphology of AZ31B, and some small dimples were exhibited at a temperature of 150 °C. With the increase in the strain rate, the quantity and size of the dimples did not obviously decrease. When the temperature was raised to 250 °C, the dimple depth in the fracture surface of AZ31B was deeper than the lower temperature, as shown in Figure 10j–l, which was the typical dimple pattern. Additionally, the better plasticity of AZ31B was exhibited under the lower strain rate at a temperature of 250 °C. Meanwhile, the deeper dimple pattern also provided evidence for the plasticity of AZ31B at the high tensile temperature. Based on the analysis of the fracture morphology of AZ31B and the mechanical properties above, with the increase in tensile temperature, the fracture pattern of AZ31B was gradually transited from a quasi-cleavage fracture pattern to a ductile fracture pattern. The cleavage step and river pattern were observed at a temperature of 25 °C; with the increasing temperature, the big and deep dimples were exhibited at a temperature of 250 °C. It was observed that the elongation percentage after the fracture and plasticity of AZ31B increased with the increasing temperature, as seen in Figure 7. This phenomenon could be attributed to the transition between the hardening effect and softening effect of AZ31B [28]. When the tensile temperature was 25 °C, a more hardening phenomenon was exhibited, and there was not enough energy to support the plasticity deformation and dislocation's rapid propagation. Therefore, the formability of AZ31B was mainly determined by its hardening during the tensile process. However, with the increase in temperature, the softening effect increased gradually. When the temperature was raised to 250 °C, there was enough energy to support the deformation and the dislocation's rapid propagation of AZ31B during the tensile process. Therefore, the plasticity and formability of AZ31B were improved at a high

temperature. However, at the same temperature, there was not enough time to support the deformation of AZ31B; thus, lower plasticity was exhibited. Therefore, at a temperature of 250 °C, the depth of the dimples at $0.017\,\mathrm{s}^{-1}$ was deeper than that at $0.34\,\mathrm{s}^{-1}$.
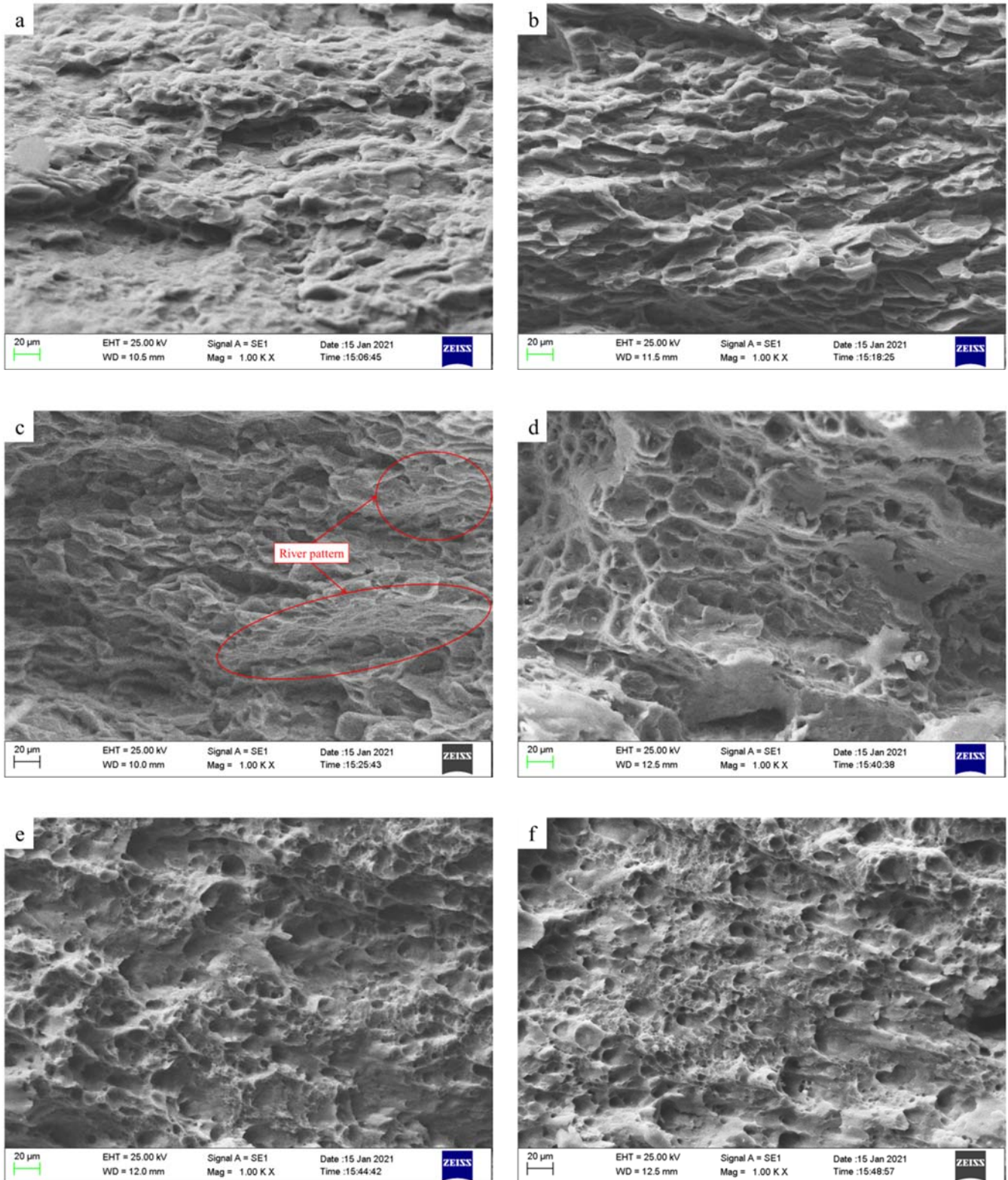

Figure 10. *Cont.*

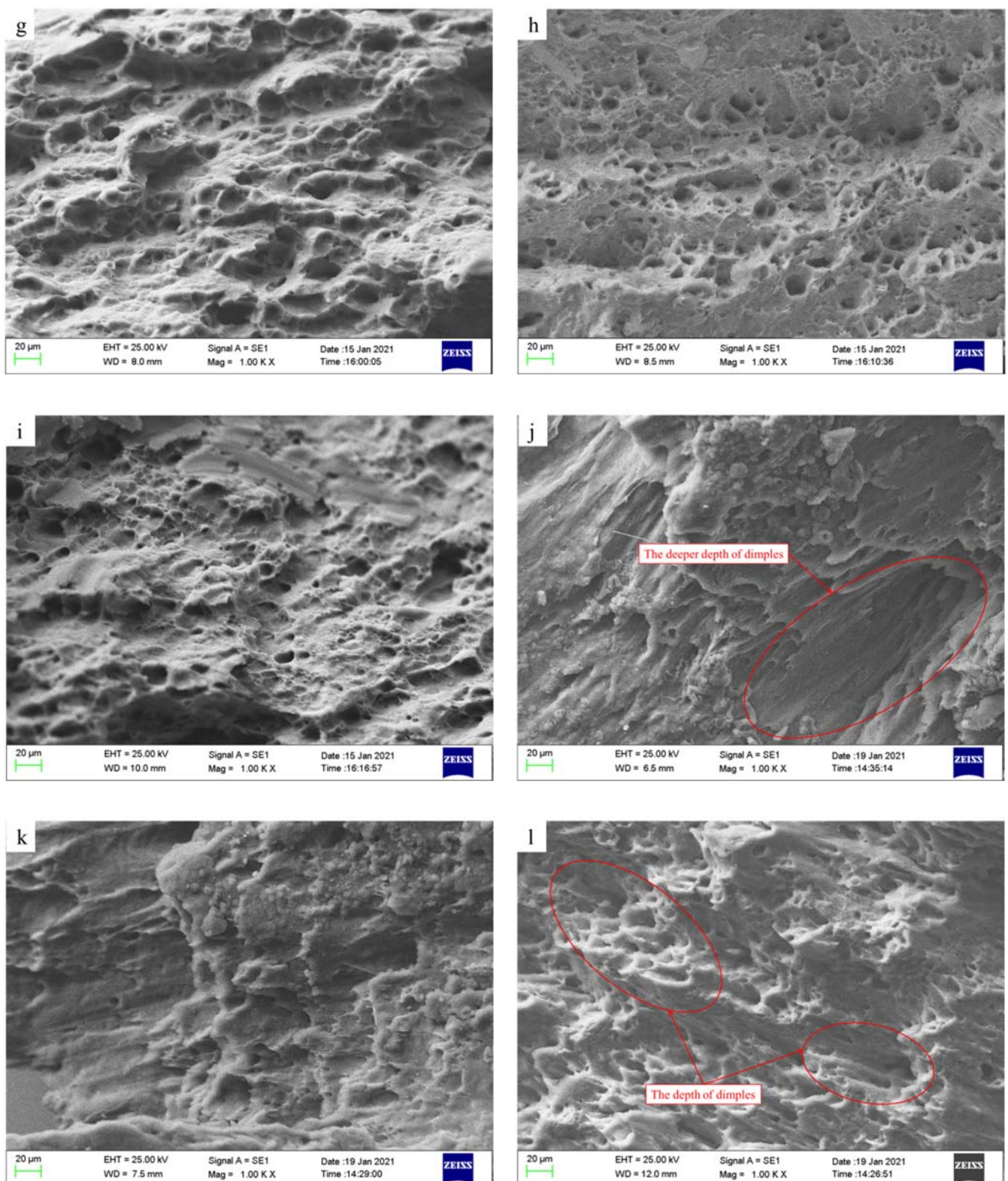**Figure 10.** The fracture morphology of AZ31B at different temperatures and strain rates. (**a**) 0.017 s^{-1} at 25 °C; (**b**) 0.17 s^{-1} at 25 °C; (**c**) 0.34 s^{-1} at 25 °C; (**d**) 0.017 s^{-1} at 150 °C; (**e**) 0.17 s^{-1} at 150 °C; (**f**) 0.34 s^{-1} at 150 °C; (**g**) 0.017 s^{-1} at 200 °C; (**h**) 0.17 s^{-1} at 200 °C; (**i**) 0.34 s^{-1} at 200 °C; (**j**) 0.017 s^{-1} at 250 °C; (**k**) 0.17 s^{-1} at 250 °C; (**l**) 0.34 s^{-1} at 250 °C.

4. Conclusions

In this article, the tensile tests for the AZ31B magnesium alloy sheet were carried out at different temperatures and strain rates. According to the analysis of the mechanical property and microstructure of AZ31B at the different strain rates and temperatures, the following results were reached:

(1) AZ31B magnesium alloy sheets behave positively to temperature sensitivity when forming at a temperature lower than 200 °C.

(2) The partially recrystallized AZ31B was exhibited at a temperature of 150 °C, and the approximate complete recrystallization was exhibited at a temperature of 250 °C. At room temperature, the quasi-cleavage fracture pattern is the main fracture pattern for AZ31B in the forming process. However, with an increasing temperature, the fracture pattern of AZ31B transits from a quasi-cleavage fracture pattern to a ductile fracture pattern in the forming process. At a high temperature, the ductile fracture pattern is the main fracture pattern for AZ31B in the forming process.

(3) The strain rate is an important factor in affecting the plasticity and formability of AZ31B. At room temperature, there is no obvious effect. However, with the increasing temperature, the distinct effect of the strain rate on the grain structure and plasticity is exhibited at a temperature of 150 °C, and a more serious effect is exhibited at a temperature of 250 °C.

(4) The percentage elongation after the fracture of AZ31B declined with the increasing strain rates. The formability and plasticity would be improved by controlling the lower strain rate and the higher temperature in the forming process.

References

1. Shen, Y.; Song, Y.; Hua, L.; Lu, J. Influence of plastic deformation on martensitic transformation during hot stamping of complex structure auto parts. *J. Mater. Eng. Perform.* **2017**, *26*, 1830–1838. [CrossRef]
2. Wang, W.; Chen, S.; Tao, K.; Gao, K.; Wei, X. Experimental investigation of limit drawing ratio for AZ31B magnesium alloy sheet in warm stamping. *Int. J. Adv. Manuf. Technol.* **2017**, *92*, 723–731. [CrossRef]
3. Song, J.; She, J.; Chen, D.; Pan, F. Latest research advances on magnesium and magnesium alloys worldwide. *J. Magnes. Alloy.* **2020**, *5*, 1–41. [CrossRef]
4. Wang, S.; Gao, G. Performance of extruded magnesium alloy AZ31B circular tubes under uniaxial compression. *Thin-Walled Struct.* **2018**, *131*, 464–474. [CrossRef]
5. Yang, Q.; Jiang, B.; Song, B.; Yu, Z.; He, D.; Chai, Y.; Zhang, J.; Pan, F. The effects of orientation control via tension-compression on microstructural evolution and mechanical behavior of AZ31 Mg alloy sheet. *J. Magnes. Alloy.* **2022**, *10*, 411–422. [CrossRef]
6. Jabbari, A.H.; Sedighi, M.; Sabet, A.S. Combination of Mechanical and Electromagnetic Stirring to Distribute Nano-Sized Al_2O_3 Particles in Magnesium Matrix Composite. *Powder Metall. Met. Ceram.* **2019**, *58*, 361–371. [CrossRef]
7. Jia, W.; Ma, L.; Le, Q.; Zhi, C.; Liu, P. Deformation and fracture behaviors of AZ31B Mg alloy at elevated temperature under uniaxial compression. *J. Alloy. Compd.* **2019**, *783*, 863–876. [CrossRef]
8. Chai, Y.; Song, Y.; Jiang, B.; Fu, J.; Jiang, Z.; Yang, Q.; Sheng, H.; Huang, G.; Zhang, D.; Pan, F. Comparison of microstructures and mechanical properties of composite extruded AZ31 sheets. *J. Magnes. Alloy.* **2019**, *7*, 545–554. [CrossRef]

9. Joost, W.J.; Krajewski, P.E. Towards magnesium alloys for high-volume automotive applications. *Scr. Mater.* **2017**, *128*, 107–112. [CrossRef]

10. You, S.; Huang, Y.; Kainer, K.U.; Hort, N. Recent research and developments on wrought magnesium alloys. *J. Magnes. Alloy.* **2017**, *5*, 239–253. [CrossRef]

11. Davies, J.R. (Ed.) *Tensile Testing*, 2nd ed.; ASM International: Materials Park, OH, USA, 2004.

12. Li, Z.; Zhou, G.; Li, D.; Jain, M.K.; Peng, Y.; Wu, P. Forming limits of magnesium alloy AZ31B sheet at elevated temperatures. *Int. J. Plast.* **2020**, *135*, 102822. [CrossRef]

13. Wang, Z.; Gu, R.; Chen, S.; Wang, W.; Wei, X. Effect of upper-die temperature on the formability of AZ31B magnesium alloy sheet in stamping. *J. Mater. Process. Technol.* **2018**, *257*, 180–190. [CrossRef]

14. Wang, W.; Huang, L.; Tao, K.; Chen, S.; Wei, X. Formability and numerical simulation of AZ31B magnesium alloy sheet in warm stamping process. *Mater. Des.* **2015**, *87*, 835–844. [CrossRef]

15. Tari, D.G.; Worswick, M.J. Elevated temperature constitutive behavior and simulation of warm forming of AZ31B. *J. Mater. Process. Technol.* **2015**, *221*, 40–55. [CrossRef]

16. Nie, X.; Ni, J.; Dong, S.; Wang, F.; Jin, L.; Dong, J. Preferential grain growth and textural evolution of AZ31B Mg alloy during annealing after isothermal compression at 400 °C. *Mater. Charact.* **2020**, *169*, 110566. [CrossRef]

17. Dong, J.-R.; Zhang, D.-F.; Dong, Y.-F.; Pan, F.-S.; Chai, S.-S. Critical damage value of AZ31B magnesium alloy with different temperatures and strain rates. *Rare Met.* **2021**, *40*, 137–142. [CrossRef]

18. Zhou, G.; Liu, R.; Tang, W.; Li, D.; Peng, Y.; Wu, P. Strain-Rate Sensitivities of Different Deformation Mechanismsin AZ31B Magnesium Alloy Sheet at Various Temperatures. *J. Electr. Microsc.* **2021**, *73*, 1419–1427. [CrossRef]

19. Wang, H.M.; Wu, P.D.; Kurukuri, S.; Worswick, M.J.; Peng, Y.H.; Tang, D.; Li, D.Y. Strain rate sensitivities of deformation mechanisms in magnesium alloys. *Int. J. Plast.* **2018**, *107*, 207–222. [CrossRef]

20. Huang, G.S.; Zhang, H.; Gao, X.Y.; Bo, S.O.N.G.; Zhang, L. Forming limit of textured AZ31B magnesium alloy sheet at different temperatures. *Trans. Nonferrous Met. Soc. China* **2011**, *21*, 836–843. [CrossRef]

21. Yu, D.-H. Modeling high-temperature tensile deformation behavior of AZ31B magnesium alloy considering strain effects. *Mater. Des.* **2013**, *51*, 323–330. [CrossRef]

22. *GB/T 228.1-2010*; Metallic Materials-Test Pieces for Tensile Testing. China Quality Inspection Press: Beijing, China, 2021.

23. Zhang, K.; Zheng, J.H.; Shao, Z.; Pruncu, C.; Turski, M.; Guerini, C.; Jiang, J. Experimental investigation of the viscoplastic behaviours and microstructure evolutions of AZ31B and Elektron 717 Mg-alloys. *Mater. Des.* **2019**, *184*, 108160. [CrossRef]

24. Dong, J.; Zhang, D.; Dong, Y.; Chai, S.; Pan, F. Microstructure evolution and mechanical response of extruded AZ31B magnesium alloy sheet at large strains followed by annealing treatment. *Mater. Sci. Eng. A* **2014**, *618*, 262–270. [CrossRef]

25. Xie, Q.; Zhu, Z.; Kang, G. Thermal activation based constitutive model for high-temperature dynamic deformation of AZ31B magnesium alloy. *Mater. Sci. Eng. A* **2019**, *743*, 24–31. [CrossRef]

26. Trojanova, Z.; Mathis, K.; Luka, P.; Nemeth, G.; Chmelik, F. Internal stress and thermally activated dislocation motion in an AZ63 magnesium alloy. *Mater. Chem. Phys.* **2011**, *130*, 1146–1150. [CrossRef]

27. Smerd, R.; Winkler, S.; Salisbury, C.; Worswick, M.; Lloyd, D.; Finn, M. High strain rate tensile testing of automotive aluminum alloy sheet. *Int. J. Impact Eng.* **2005**, *32*, 541–560. [CrossRef]

28. Liu, H.Q.; Pang, J.C.; Wang, M.; Li, S.X.; Zhang, Z.F. Effect of high temperature on the mechanical properties of Al–Si–Cu–Mg–Ni–Ce alloy. *Mater. Sci. Eng. A* **2021**, *824*, 141762. [CrossRef]